# Circulating Current Elimination of Grid-Connected Modular Multilevel Converters

Fatemeh Shahnazian, Jafar Adabi
Babol (Noshirvani) Univ. Technology, Iran
f_shahnazian@yahoo.com; j.adabi@nit.ac.ir

Edris Pouresmaeil
Dep. of Elec. Eng. and Auto., Aalto University, Finland
edris.pouresmaeil@gmail.com

Majid Mehrasa
C-MAST/UBI, Covilha, Portugal
m.majidmehrasa@gmail.com

João P. S. Catalão
INESC TEC and FEUP, Porto, C-MAST/UBI, Covilha, and INESC-ID/ IST-UL, Lisbon, Portugal
catalao@fe.up.pt

***Abstract*—This paper presents an analytical dynamic model of a modular multilevel converter (MMC) in grid-connected operating mode. The proposed model is then efficiently used to design a circulating current controller. The proposed controller can accurately study the dynamic and steady-state performance of the converter through harmonic evaluations. Based on this configuration, the modulation is accomplished so that the stable performance of the converter in the network is obtained, which is considered as the foremost novelty of the proposed control method over existing control methods. In order to mitigate the circulating currents, the proposed controller inserts an estimated second harmonic component into modulation indices, which is considered as the second novelty of the proposed control method. The functionality and capability of the proposed control method are validated using detailed theoretical analysis and simulations with MATLAB/Simulink.**

***Keywords— circulating current control; improved steady-state operation; modular multilevel converter (MMC).***

## I. INTRODUCTION

Modular multilevel converters (MMCs) have attracted considerable attention in medium/high voltage applications over the past decade. This is mainly due to the MMCs' exclusive structural features such as simple scalability to higher voltage levels, high-quality output voltage, less filter expenses, lower switching frequency and reduced converter losses. These advantages have made MMCs the preferred structure over conventional voltage source converters (VSCs), especially in high voltage direct current (HVDC) and motor drive applications [1]-[2].

New non-linear MMC modeling techniques need a huge amount of simulation time due to their detailed, discrete nature. To resolve these technical issues average models are presented [1]. Despite being accurate and efficient, both models are represented in abc frame which is not convenient for imbalance transient studies and controller design [3]. This highlights the need for dq frame models as they are more compatible with desired controllers.

Among the various aspects such as capacitor voltage balancing [4] and fault tolerance [5], that should be controlled to achieve stable performance, circulating current suppression is a matter of great importance in MMCs. Circulating current flows inside the converter due to voltage differences between dc link and converter legs [3].

J.P.S. Catalão acknowledges the support by FEDER funds through COMPETE 2020 and by Portuguese funds through FCT, under Projects SAICT-PAC/0004/2015 - POCI-01-0145-FEDER-016434, POCI-01-0145-FEDER-006961, UID/EEA/50014/2013, UID/CEC/50021/2013, UID/EMS/00151/2013, 02/SAICT/2017 - POCI-01-0145-FEDER-029803, and also funding from the EU 7th Framework Programme FP7/2007-2013 under GA no. 309048.

Despite having no impact on output voltages and currents, circulating currents should be eliminated as they increase rms values of arm currents, the ratings of power devices, capacitor voltage fluctuations and converter losses [6].

Increasing the value of arm inductors to limit the circulating currents seems to be inefficient and yet costly [3]. Therefore, various controllers have been individually designed for this purpose [7]-[8]. One approach is to focus on reducing harmonic components, which leads to a slower dynamic response [9]. Enhanced methods based on quasi-proportional resonant (quasi-PR) controllers propose a more detailed dc and harmonic reference follow along with improved transient response [10]. These controllers are usually designed to cope with a limited order of harmonics as the controller complexity grows with accuracy. To reduce complexity, [11] proposes a circulating current control through redundant voltage levels of the converter. Defining the number of selected sub-modules (SMs) in the modulation process, this procedure eliminates additional control loops and improves converter dynamics especially at large numbers of SMs. Reference [12] presents a repetitive control to eliminate even-harmonic components of circulating current. The proposed technique occupies less memory for data processing which leads to less delay compared to conventional closed-loop controllers. The greatest weakness of aforementioned methods is their ineffectiveness in imbalance studies.

This paper presents a dynamic model of MMCs in dq frame as it is more convenient than abc models for stability analysis purposes as well as controller design. Based on this accurate model, modulation indices are obtained which is considered as a novelty of this paper. Moreover, a circulating current control is proposed according to second harmonic expressions of the model as the second novelty of this paper. The coordination between converter model and the proposed controller guarantees stable performance of the MMCs in a grid-connected operating mode.

## II. GENERAL STRUCTURE OVERVIEW AND THE PROPOSED DYNAMIC MODEL

The most common configuration of a three-phase grid-connected MMC converter is presented in Fig. 1(a). Each phase leg consists of upper and lower arms which contain N series-connected SMs, one arm inductor $L_{arm}$, and one parasitic resistance $R_{arm}$.

978-1-5386-5186-5/18/$31.00 ©2018 IEEE

Known as the general configuration of SMs, half-bridges consist of IGBT switches and dc capacitors as shown in Fig. 1(b). The voltages inserted by each upper and lower arm (specified by *u* and *l* correspondingly) can be represented as $U_{cux} = n_{ux}U^{\Sigma}_{cux}$ and $U_{clx} = n_{lx}U^{\Sigma}_{clx}$, $x = a,b,c$ in which modulation indices ($n_{ux}, n_{lx}$) and sum capacitor voltages ($U^{\Sigma}_{cux}, U^{\Sigma}_{clx}$) contain dc, fundamental, and second harmonic components. Thus, the aforementioned quantities can be expressed as follows:

$$\begin{aligned} n_{ux} &= \frac{1 - m_{1x}\cos(\omega t - \theta_{m1}) - m_{2x}\cos(2\omega t - \theta_{m2})}{2} \\ &\equiv \left(\frac{1}{2}\right) + \left(\frac{-m_d}{2}\right)\cos(\omega t) + \left(\frac{-m_q}{2}\right)\sin(\omega t) \\ &\quad + \left(\frac{-m_{d2}}{2}\right)\cos(2\omega t) + \left(\frac{-m_{q2}}{2}\right)\sin(2\omega t) \end{aligned} \quad (1)$$

$$\begin{aligned} n_{lx} &= \frac{1 + m_{1x}\cos(\omega t - \theta_{m1}) - m_{2x}\cos(2\omega t - \theta_{m2})}{2} \\ &\equiv \left(\frac{1}{2}\right) + \left(\frac{m_d}{2}\right)\cos(\omega t) + \left(\frac{m_q}{2}\right)\sin(\omega t) \\ &\quad + \left(\frac{-m_{d2}}{2}\right)\cos(2\omega t) + \left(\frac{-m_{q2}}{2}\right)\sin(2\omega t) \end{aligned} \quad (2)$$

$$\begin{aligned} U^{\Sigma}_{cux}(t) &= U^{\Sigma}_{cum0} + U^{\Sigma}_{cum1}\cos(\omega t - \theta_u) + U^{\Sigma}_{cum2}\cos(2\omega t - \theta_{u2}) \\ &\equiv U^{\Sigma}_{cu0} + U^{\Sigma}_{cud} + U^{\Sigma}_{cuq} + U^{\Sigma}_{cud2} + U^{\Sigma}_{cuq2} \end{aligned} \quad (3)$$

$$\begin{aligned} U^{\Sigma}_{clx}(t) &= U^{\Sigma}_{clm0} + U^{\Sigma}_{clm1}\cos(\omega t - \theta_l) + U^{\Sigma}_{clm2}\cos(2\omega t - \theta_{l2}) \\ &\equiv U^{\Sigma}_{cl0} + U^{\Sigma}_{cld} + U^{\Sigma}_{clq} + U^{\Sigma}_{cld2} + U^{\Sigma}_{clq2} \end{aligned} \quad (4)$$

where the fundamental frequency components at $\omega = 2\pi f$ are represented by subscripts *d* and *q*, whereas subscripts *d2,q2 and 0* denote the second harmonic and zero sequence components respectively.

Following that, based on Fig. 1(a), each arm current ($i_{ux}$, $i_{lx}$) can be represented as:

$$i_{ux} = i_{circx} + \frac{i_x}{2} \quad (5)$$

$$i_{lx} = i_{circx} - \frac{i_x}{2} \quad (6)$$

where, $i_x$ represents the fundamental frequency current in phase *x* while $i_{circx}$ represents the circulating current of leg *x*, consisting of dc and second harmonic components.

Considering the energy stored in SM capacitors used in each arm, following dynamics of the sum capacitor voltages are obtained as:

$$\frac{dW^{\Sigma}_{cu,l}}{dt} = \frac{d}{dt}\left(\frac{1}{2}\frac{C}{N}\left(U^{\Sigma}_{cu,l}\right)^2\right) = \frac{C}{N}\left(U^{\Sigma}_{cu,l}\right)\left(\frac{dU^{\Sigma}_{cu,l}}{dt}\right) = \left(U_{cu,l}\right)\left(i_{u,l}\right) \quad (7)$$

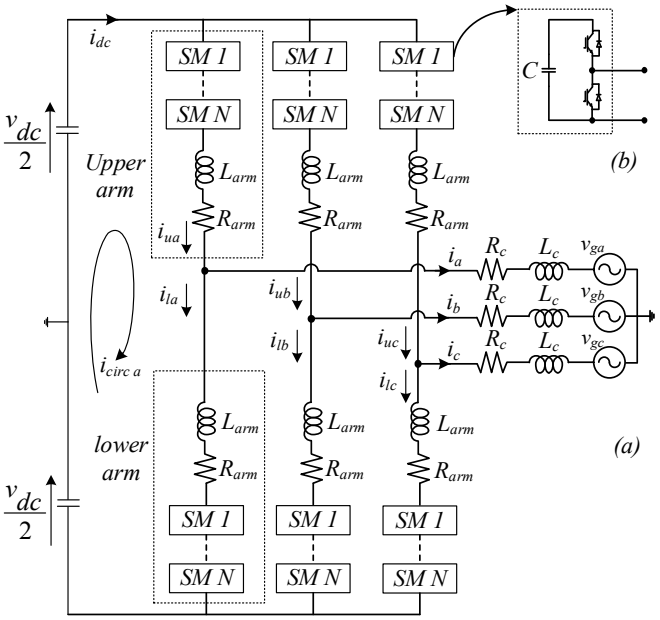


Fig. 1. General configuration of a grid-connected MMC, (a) Circuit schematic, (b) SM structure.

where the energy derivative equals the power injected into each arm. Substituting $U_{cu,l} = n_{u,l}U^{\Sigma}_{cu,l}$, (8) can be represented as:

$$\begin{cases} \frac{C}{N}\frac{dU^{\Sigma}_{cux}}{dt} = n_{ux}i_{ux} \\ \frac{C}{N}\frac{dU^{\Sigma}_{clx}}{dt} = n_{lx}i_{lx} \end{cases} \quad (8)$$

Finally, considering harmonic components of each parameter leads to the dq0 frame representation of the aforementioned equation as follows:

$$\begin{aligned} \frac{C}{N}\frac{d}{dt}\begin{bmatrix} U^{\Sigma}_{cud} \\ U^{\Sigma}_{cuq} \\ U^{\Sigma}_{cud2} \\ U^{\Sigma}_{cuq2} \\ U^{\Sigma}_{cu0} \end{bmatrix} &= \frac{C}{N}\begin{bmatrix} 0 & \omega & 0 & 0 & 0 \\ -\omega & 0 & 0 & 0 & 0 \\ 0 & 0 & 0 & 2\omega & 0 \\ 0 & 0 & -2\omega & 0 & 0 \\ 0 & 0 & 0 & 0 & 0 \end{bmatrix}\begin{bmatrix} U^{\Sigma}_{cud} \\ U^{\Sigma}_{cuq} \\ U^{\Sigma}_{cud2} \\ U^{\Sigma}_{cuq2} \\ U^{\Sigma}_{cu0} \end{bmatrix} \\ &+ \begin{bmatrix} -\frac{m_d}{2}i_{uo} + \frac{1}{2}i_{ud} - \frac{m_{d2}}{4}i_{ud} - \frac{m_{q2}}{4}i_{uq} - \frac{m_d}{4}i_{ud2} - \frac{m_q}{4}i_{uq2} \\ -\frac{m_q}{2}i_{uo} + \frac{1}{2}i_{uq} + \frac{m_{d2}}{4}i_{uq} - \frac{m_{q2}}{4}i_{ud} + \frac{m_q}{4}i_{ud2} - \frac{m_d}{4}i_{uq2} \\ -\frac{m_d}{4}i_{ud} + \frac{m_q}{4}i_{uq} - \frac{m_{d2}}{2}i_{u0} + \frac{1}{2}i_{ud2} \\ -\frac{m_q}{4}i_{ud} - \frac{m_d}{4}i_{uq} - \frac{m_{q2}}{2}i_{u0} + \frac{1}{2}i_{uq2} \\ \frac{1}{2}i_{u0} - \frac{m_d}{4}i_{ud} - \frac{m_q}{4}i_{uq} - \frac{m_{d2}}{4}i_{ud2} - \frac{m_{q2}}{4}i_{uq2} \end{bmatrix} \end{aligned} \quad (9)$$

On the other hand, considering $i_x = i_{ux} - i_{lx}$ and applying KVL to Fig. 1(a) leads to:

$$\begin{aligned}&(L_c + L_{arm})\frac{di_{ux}}{dt} - L_c\frac{di_{lx}}{dt} = -(R_c + R_{arm})i_{ux} + R_c i_{lx} \\ &-v_{gx} + \frac{v_{dc}}{2} - n_{ux}U^{\Sigma}_{cux}\end{aligned} \tag{10}$$

Finally, considering (1)-(4), the dynamic equation of the MMC could be expressed in dq0 frame as:

$$\begin{aligned}&(L_c + L_{arm})\frac{d}{dt}\begin{bmatrix} i_{ud} \\ i_{uq} \\ i_{uo}\end{bmatrix} - L_c\frac{d}{dt}\begin{bmatrix} i_{ld} \\ i_{lq} \\ i_{lo}\end{bmatrix} = \\ &\begin{bmatrix} -(R_c + R_{arm}) & (L_c + L_{arm})\omega & 0 \\ -(L_c + L_{arm})\omega & -(R_c + R_{arm}) & 0 \\ 0 & 0 & -(R_c + R_{arm})\end{bmatrix}\begin{bmatrix} i_{ud} \\ i_{uq} \\ i_{uo}\end{bmatrix} \\ &+\begin{bmatrix} R_c & -L_c\omega & 0 \\ L_c\omega & R_c & 0 \\ 0 & 0 & R_c\end{bmatrix}\begin{bmatrix} i_{ld} \\ i_{lq} \\ i_{lo}\end{bmatrix} - \begin{bmatrix} v_{gd} \\ v_{gq} \\ 0\end{bmatrix} + \begin{bmatrix} 0 \\ 0 \\ \frac{v_{dc}}{2}\end{bmatrix} \\ &-\begin{bmatrix} -\frac{m_d}{2}U^{\Sigma}_{cu0} + \frac{1}{2}U^{\Sigma}_{cud} - \frac{m_{d2}}{4}U^{\Sigma}_{cud} - \frac{m_{q2}}{4}U^{\Sigma}_{cuq} - \frac{m_d}{4}U^{\Sigma}_{cud2} - \frac{m_q}{4}U^{\Sigma}_{cuq2} \\ -\frac{m_q}{2}U^{\Sigma}_{cu0} + \frac{1}{2}U^{\Sigma}_{cuq} + \frac{m_{d2}}{4}U^{\Sigma}_{cuq} - \frac{m_{q2}}{4}U^{\Sigma}_{cud} + \frac{m_q}{4}U^{\Sigma}_{cud2} - \frac{m_d}{4}U^{\Sigma}_{cuq2} \\ \frac{1}{2}U^{\Sigma}_{cu0} - \frac{m_d}{4}U^{\Sigma}_{cud} - \frac{m_q}{4}U^{\Sigma}_{cuq} - \frac{m_{d2}}{4}U^{\Sigma}_{cud2} - \frac{m_{q2}}{4}U^{\Sigma}_{cuq2}\end{bmatrix}\end{aligned} \tag{11}$$

## III. Steady- State Performance Studies of the Suggested MMC Model

To evaluate modulation indices for the steady-state performance of MMC, all quantities of previous equations should be substituted by their reference amounts. Therefore, all derivative components in (9) are substituted by zero. Also, $i_{ud2}$ and $i_{uq2}$ as well as $m_{d2}$ and $m_{q2}$ are neglected due to the designed controllers while zero component of sum capacitor voltages ($U^{\Sigma}_{cu0}$) is considered equal to the reference voltage amount of dc-link ($V_r$). This way, steady-state values of sum capacitor voltages can be derived from (9).

In order to obtain the best operation during transients, the instantaneous deviations in reference amounts of each arm current are considered in the controller. Consequently:

$$\begin{aligned}&\frac{di_{ud}}{dt} = I^*_{avud} = \frac{I^*_{avd}}{2}\ ,\ \frac{di_{uq}}{dt} = I^*_{avuq} = \frac{I^*_{avq}}{2}\ , \\ &\frac{di_{ld}}{dt} = I^*_{avld} = -\frac{I^*_{avd}}{2}\ ,\ \frac{di_{lq}}{dt} = I^*_{avlq} = -\frac{I^*_{avq}}{2}\end{aligned} \tag{12}$$

Also, instantaneous values of arm currents should be substituted by their reference amounts as follows:

$$\begin{aligned}&i_{ud} = I^*_{ud} = \frac{I^*_d}{2}\ ,\ i_{uq} = I^*_{uq} = \frac{I^*_q}{2}\ ,\ i_{ld} = I^*_{ld} = -\frac{I^*_d}{2}\ , \\ &i_{lq} = I^*_{lq} = -\frac{I^*_q}{2},\ i_{u0} = i_{l0} = I^*_0\end{aligned} \tag{13}$$

Thus, applying the aforementioned assumptions to (11), steady-state operation equations for the suggested dynamic model can be represented as follows:

$$\begin{aligned}&\begin{bmatrix} L_c + \frac{L_{arm}}{2} & 0 & 0 \\ 0 & L_c + \frac{L_{arm}}{2} & 0 \\ \frac{m_{ds}}{4}L_{arm} & \frac{m_{qs}}{4}L_{arm} & 0\end{bmatrix}\begin{bmatrix} I^*_{avd} \\ I^*_{avq} \\ V_r\end{bmatrix} = -\begin{bmatrix} V^*_{gd} \\ V^*_{gq} \\ 0\end{bmatrix} + \\ &\begin{bmatrix} -\left(R_c + \frac{R_{arm}}{2}\right) & \left(L_c + \frac{L_{arm}}{2}\right)\omega + \frac{N\left(3m^2_{qs} - m^2_{ds} - 8\right)}{64C\omega} & \frac{m_{ds}}{2} \\ -\left(L_c + \frac{L_{arm}}{2}\right)\omega - \frac{N\left(3m^2_{ds} - m^2_{qs} - 8\right)}{64C\omega} & -\left(R_c + \frac{R_{arm}}{2}\right) & \frac{m_{qs}}{2} \\ -\frac{8m_{ds}C\omega R_{arm} + 2Nm_{qs}}{32C\omega} & -\frac{8m_{qs}C\omega R_{arm} - 2Nm_{ds}}{32C\omega} & 0\end{bmatrix}\begin{bmatrix} I^*_d \\ I^*_q \\ V_r\end{bmatrix}\end{aligned} \tag{14}$$

Last row of (14) leads to:

$$\underbrace{m_{ds}\left(\frac{L_{arm}}{4}I^*_{avd} + \frac{R_{arm}}{4}I^*_d - \frac{N}{16C\omega}I^*_q\right)}_{A} = \underbrace{m_{qs}\left(-\frac{L_{arm}}{4}I^*_{avq} - \frac{R_{arm}}{4}I^*_q - \frac{N}{16C\omega}I^*_d\right)}_{B} \tag{15}$$

It is evident that both $A$ and $B$ have constant values. Thus (15) states a linear proportion between $m_{ds}$ and $m_{qs}$.

In this regard, first row of (14) leads to a quadratic equation which can be expressed in terms of $m_{ds}$ as follows:

$$\begin{aligned}&\frac{\left(3NA^2 - B^2\right)I^*_q}{64C\omega B^2}m^2_{ds} + \frac{V_r}{2}m_{ds} = V^*_{gd} + (L_c + \frac{L_{arm}}{2})I^*_{avd} \\ &+\left(R_c + \frac{R_{arm}}{2}\right)I^*_d - (L_c + \frac{L_{arm}}{2})\omega I^*_q + \frac{1}{8C\omega}I^*_q\end{aligned} \tag{16}$$

By solving the expressed quadratic equation in (16), $m_{ds}$ and $m'_{ds}$ can be expressed as (17). Therefore, $m_{qs}$ and $m'_{qs}$ can also be derived based on (15).

$$
\begin{cases}
m_{ds} = \dfrac{-16C\omega B^2 V_r}{\left(3NA^2 - B^2\right) I_q^*} + \\
\dfrac{\sqrt{\dfrac{V_r^2}{4} - \left(\dfrac{\left(3NA^2 - B^2\right) I_q^*}{16C\omega B^2}\right)\left(V_{gd}^* + (L_c + \dfrac{L_{arm}}{2}) I_{avd}^* + \left(R_c + \dfrac{R_{arm}}{2}\right) I_d^* - (L_c + \dfrac{L_{arm}}{2}) \omega I_q^* + \dfrac{1}{8C\omega} I_q^*\right)}}{\dfrac{\left(3NA^2 - B^2\right) I_q^*}{32C\omega B^2}} \\
m_{ds}^{'} = \dfrac{-16C\omega B^2 V_r}{\left(3NA^2 - B^2\right) I_q^*} - \\
\dfrac{\sqrt{\dfrac{V_r^2}{4} - \left(\dfrac{\left(3NA^2 - B^2\right) I_q^*}{16C\omega B^2}\right)\left(V_{gd}^* + (L_c + \dfrac{L_{arm}}{2}) I_{avd}^* + \left(R_c + \dfrac{R_{arm}}{2}\right) I_d^* - (L_c + \dfrac{L_{arm}}{2}) \omega I_q^* + \dfrac{1}{8C\omega} I_q^*\right)}}{\dfrac{\left(3NA^2 - B^2\right) I_q^*}{32C\omega B^2}}
\end{cases}
\tag{17}
$$

## IV. Circulating Current Controller

Circulating currents are produced because of the voltage deviations between dc-link and each phase leg. These currents include a dc component which is responsible for dc to ac power exchange and a second harmonic part with no effect on the outer dynamic of the converter. The harmonic term results in an increment in the *rms* value of each arm current as well as power dissipations and therefore, should be eliminated. Considering $\theta = 2\omega t$, the phase sequence of the transformation to the rotational frame would be a-*c*-*b*. Therefore, the KVL applied in each phase loop of the converter can be expressed as follows:

$$
L_{arm} \frac{d}{dt}\begin{bmatrix} i_{ud\,2} \\ i_{uq\,2} \end{bmatrix} = \begin{bmatrix} -R_{arm} & 2L_{arm}\,\omega \\ -2L_{arm}\,\omega & -R_{arm} \end{bmatrix}\begin{bmatrix} i_{ud\,2} \\ i_{uq\,2} \end{bmatrix}
$$
$$
-\begin{bmatrix} -\dfrac{m_d}{4}U_{cud}^{\Sigma} + \dfrac{m_q}{4}U_{cuq}^{\Sigma} - \dfrac{m_{d\,2}}{2}U_{cu\,0}^{\Sigma} + \dfrac{1}{2}U_{cud\,2}^{\Sigma} \\ -\dfrac{m_q}{4}U_{cud}^{\Sigma} - \dfrac{m_d}{4}U_{cuq}^{\Sigma} - \dfrac{m_{q\,2}}{2}U_{cu\,0}^{\Sigma} + \dfrac{1}{2}U_{cuq\,2}^{\Sigma} \end{bmatrix} \tag{18}
$$

In order to provide the stable performance of MMC, the second harmonic components of currents are preferred to become zero. Second harmonic quantities of modulation indices should be calculated and then inclined to zero.

$$
m_{d2s} = \frac{2}{U_{cu0}^{\Sigma}}\left[L_{arm}\frac{d}{dt}i_{ud2} + R_{arm}i_{ud2} - 2L_{arm}\omega i_{uq2} - \frac{m_{ds}}{4}U_{cud}^{\Sigma} + \frac{m_{qs}}{4}U_{cuq}^{\Sigma} + \frac{1}{2}U_{cud2}^{\Sigma}\right] \tag{19}
$$

$$
m_{q2s} = \frac{2}{U_{cu0}^{\Sigma}}\left[L_{arm}\frac{d}{dt}i_{uq2} + R_{arm}i_{uq2} + 2L_{arm}\omega i_{ud2} - \frac{m_{qs}}{4}U_{cud}^{\Sigma} - \frac{m_{ds}}{4}U_{cuq}^{\Sigma} + \frac{1}{2}U_{cuq2}^{\Sigma}\right] \tag{20}
$$

Including PIs, the circulating current control eliminates second harmonic currents and improves the performance of MMC.

## V. Results and Discussion

The structure presented in Fig. 2 is simulated in MATLAB/Simulink to validate the performance of the suggested controller applied to grid-connected MMCs. The values for various circuit components as well as operational conditions used in simulations are presented in Table I.

Fig. 3(a) represents the modulation index of the upper arm of phase-a ($n_{ua}$), produced by the suggested modulation technique. In this regard, a modulation method based on phase opposition disposition (POD) carriers is applied where separate triangular carrier signal are used for each SM. The inner emf in each phase can be defined based on inserted voltages of each arm as $e_x = \dfrac{U_{clx} - U_{cux}}{2}$. Applying the above PWM pattern to switching functions of each phase, output currents of the converter are driven by the emfs illustrated in Fig. 3(b).

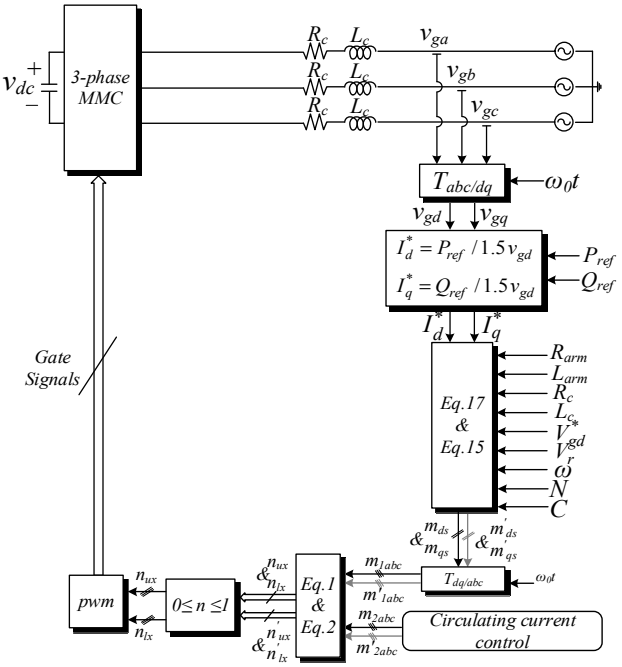


Fig. 2. General configuration of the proposed control method used in simulations.

TABLE I
MMC Component values and Operating Conditions Used in Simulations

| Items | Values |
|---|---|
| Active power $P_{ref}$ | 14 MW |
| Reactive power $Q_{ref}$ | 6 MVAr |
| ac system voltage $V_g^*$ (L-L,rms) | 10 kV |
| ac system inductance $L_c$ | 30 mH |
| ac system resistance $R_c$ | 0.5 Ω |
| dc bus voltage $V_r$ | 20 kV |
| Number of SMs per arm N | 20 |
| SM capacitance C | 10000 μF |
| Arm inductance $L_{arm}$ | 9 mH |
| Arm equivalent resistance $R_{arm}$ | 0.7 Ω |
| SM capacitor voltage $V_{csm}$ | 1 kV |
| Carrier frequency $f_{sw}$ | 5 kHz |

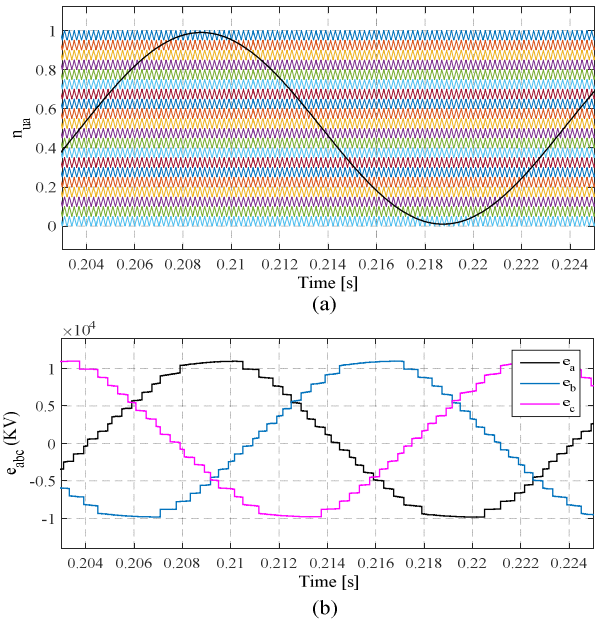


Fig. 3. Applied modulation technique, (a) modulation index of the upper arm in phase-a produced by the suggested modulation technique, (b) inner emfs in phase legs.

In order to validate the suggested circulating current controller, as shown in Fig. 4(a), the proposed algorithm is disabled initially and then enabled at 0.4 s. It is obvious that by adding appropriate components produced by the proposed controller to the modulation indices, the harmonic part of the circulating current is reduced effectively. This method provides a lower distortion in arm current, leading to a more sinusoidal waveform. Fig. 4(b) demonstrates the current waveform of the upper arm in phase-a. Note that the existence of a dc term in each arm current represents the active power transmission between the dc and ac sides and thus is necessary. Fig. 4(c) illustrates SM capacitor voltages in the upper arm of phase-a. Being in the convenient criteria, the voltages are considered to be well balanced. Also, it can be seen that the capacitor voltage fluctuations are reduced significantly. Output voltages and currents of MMC are demonstrated in Fig. 4(d) and Fig. 4(e), respectively. Considering circulating currents as interior components, the exterior dynamic operations of the MMC should not be affected by the proposed controller. In this regard, the ac-side voltages and currents appear to remain very similar and without any major changes.

## VI. Conclusion

A dynamic model of a grid-connected MMC was presented in this paper. Detailed harmonic representation of the model in dq frame provided an accurate control method for three-phase connection of the converter to the grid. Using steady-state expressions of the converter model, modulation indices were provided based on network and converter parameters, which was considered as the foremost novelty of this paper. Also, comprehensive simulations with MATLAB/Simulink have been used to validate the functionality of the proposed controller. Applying the circulating current control, a second harmonic reference has been developed and then inserted into the modulation process, which was considered as the second contribution of this paper. It has been shown that the second harmonic components of the circulating currents can be effectively suppressed, which then results in a more sinusoidal arm current. SM capacitor voltage fluctuations have also decreased significantly, leading to an enhanced output voltage quality.

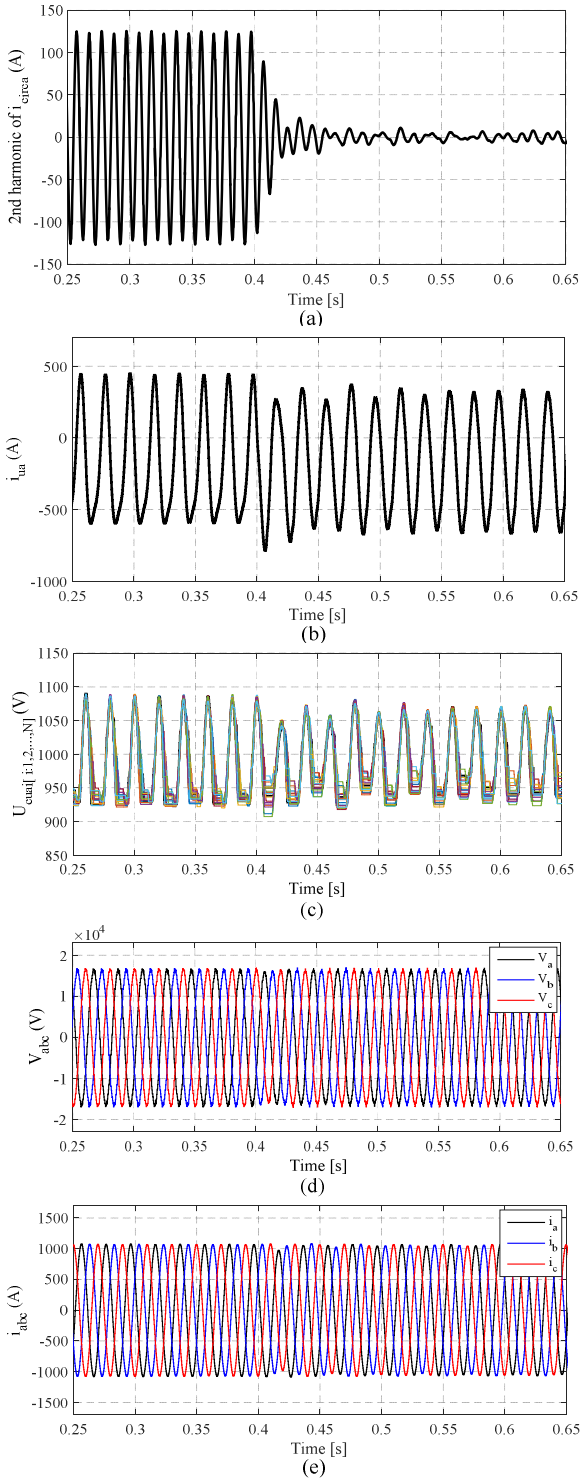


Fig. 4. Simulation results of the MMC operation with circulating current control: (a) second harmonic component of the circulating current, (b) upper arm current of phase-a, (c) upper arm SM capacitor voltages of phase-a, (d) output voltages of MMC, and (e) output currents of MMC.

## REFERENCES


[1] M. Mehrasa, E. Pouresmaeil, S. Zabihi and J. P. S. Catalao, "Dynamic model, control and stability analysis of MMC in HVDC transmission systems," IEEE Transaction on Power Delivery, vol. 32, no. 3, pp. 1471-1482, Jun. 2017.

[2] M. Mehrasa, E. Pouresmaeil, S. Zabihi, I. Vechiu, and J. P. S. Catalao, "A Multi-Loop Control Technique for the Stable Operation of Modular Multilevel Converters in HVDC Transmission Systems," International Journal of Electrical Power and Energy Systems, vol. 96, pp.194-207, Mar. 2018.

[3] J. W. Moon, C. S. Kim, J. W. Park, D. W. Kang, and J. M. Kim, "Circulating current control in MMC under the unbalanced voltage," IEEE Trans. Power Delivery, vol. 28, pp. 1952-1959, June. 2013.

[4] M. Vasiladiotis, N. Cherix, and A. Rufer, "Accurate capacitor voltage ripple estimation and current control considerations for grid-connected modular multilevel converters," IEEE Trans. Power Electronics, vol. 29, pp. 4568-4579, Sept. 2014.

[5] T. Geyer, and S. Schröder, "Reliability considerations and fault-handling strategies for multi-MW modular drive systems," IEEE Trans. Industry Applications, vol. 46, pp. 2442-2451, Nov.-Dec. 2010.

[6] F. Shahnazian, J. Adabi, E. Pouresmaeil, and J. P. S. Catalao, "Interfacing Modular Multilevel Converters for Grid Integration of Renewable Energy Sources," Electric Power Systems Research, vol. 160, pp. 439-449, Jul. 2018.

[7] M. Mehrasa, E. Pouresmaeil, S. Taheri, I. Vechiu, and J. P. S. Catalao, "Novel Control Strategy for Modular Multilevel Converters Based on Differential Flatness Theory," IEEE Jour. of Emerg. and Selected Topics in Power Electronics, (https://doi.org/10.1109/JESTPE.2017.2766047).

[8] M. Mehrasa, E. Pouresmaeil, M. F. Akorede, S. Zabihi, and J. P. S. Catalao, "Function-Based Modulation Control for Modular Multilevel Converters Under Varying Loading and Parameters Conditions," IET Gene., Trans. & Dist., vol. 11, no. 13, pp. 3222-3230, Sep. 2017.

[9] R. Darus, J. Pou, G. Konstantinou, S. Ceballos, and V. G. Agelidis, "Controllers for eliminating the ac components in the circulating current of modular multilevel converters," IET Power Electronics, vol. 9, pp. 1-8, Feb. 2016.

[10] S. Geng, Y. Gan, Y. Li, L. Hang, and G. Li, " Novel circulating current suppression strategy for MMC based on quasi-PR controller," in Proc. IEEE Applied Power Electronics Conf., pp. 3560-3565, 2016.

[11] G. Konstantinou, J. Pou, S. Ceballos, R. Picas, J. Zaragoza, and V. G. Agelidis, "Control of circulating currents in modular multilevel converters through redundant voltage levels," IEEE Trans. Power Electronics, vol. 31, no. 11, pp. 7761-7769, Nov. 2016.

[12] S. Yang, P. Wang, Y. Tang, M. Zagrodnik, X. Hu, and K. J. Tseng, " Even-harmonic repetitive control for circulating current suppression in modular multilevel converters," in Proc. IEEE Applied Power Electronics Conf., pp. 3591-3597, 2016.